Integrating Impedance Spectroscopy and Perceptron-Based Classification for Tooth Treatment Monitoring

Integrating Impedance Spectroscopy and Perceptron-Based Classification for Tooth Treatment Monitoring

Isabella Sannino
Politecnico di Torino
Turin, Italy
isabella.sannino@polito.it

Leila Es Sebar
Politecnico di Torino
Turin, Italy
leila.essebar@polito.it

Luca Lombardo
Politecnico di Torino
Turin, Italy
luca.lombardo@polito.it

Marco Parvis
Politecnico di Torino
Turin, Italy
marco.parvis@polito.it

Allegra Comba
Università degli Studi di Torino
Turin, Italy
allegra.comba@unito.it

Nicola Scotti
Università degli Studi di Torino
Turin, Italy
nicola.scotti@unito.it

Emma Angelini
Politecnico di Torino
Turin, Italy
emma.angelini@polito.it

Sabrina Grassini
Politecnico di Torino
Turin, Italy
sabrina.grassini@polito.it

***Abstract*—The increasing prevalence of dental caries necessitates the development of advanced diagnostic tools that can accurately assess the stages of tooth demineralization and the efficacy of remineralization treatments. This study introduces a novel, non-invasive procedure using impedance spectroscopy coupled with an automatic classification algorithm based on a single perceptron topology to evaluate the demineralization and remineralization states of enamel. In-vitro experimental treatments were conducted on sound human dental samples, subjected to controlled demineralization and subsequent remineralization processes, employing cutting-edge nanoparticles designed to mimic natural remineralization mechanisms. The impedance measurement, known for its sensitivity to changes in electrical properties, was adapted to detect variations in the enamel's structure and composition, indicative of demineralization and remineralization. The perceptron-based classifier was able to properly differentiate between the various stages of enamel integrity showing quite promising results. The effectiveness and accuracy of the impedance spectroscopy and classification approach were further validated by Scanning Electron Microscopy and Raman spectroscopy analyses, which confirmed the morphological and chemical modifications within the enamel. These results not only validate the proposed method as a reliable tool for early detection of dental demineralization but also offer a promising approach for monitoring the effectiveness of remineralization therapies, thereby contributing to preventive dentistry and enhanced oral health care.**

***Index Terms*—Impedance spectroscopy, multilayer perceptron, tooth characterization, tooth remineralization, carious lesions.**

I. Introduction

Diagnostic management plays a crucial role in dental treatment, directly influencing critical decisions on whether to observe or proceed with invasive procedures. Dental caries remains a prevalent challenge in oral health, affecting a significant portion of the global population across all age groups [1]. The early detection and accurate assessment of tooth demineralization and the effectiveness of remineralization treatments are critical for preventing the progression of caries and promoting oral health. Traditional diagnostic methods, including visual assessments and radiography, while widely used, have limitations in sensitivity and specificity, especially in the detection of early-stage demineralization. These methods usually rely on the operator's interpretations and expertise, and may not provide sufficient sensitivity to detect subtle enamel changes. Additionally, the need for invasive procedures or exposure to ionizing radiation in certain diagnostic approaches poses challenges in patient compliance and overall safety [2].

In recent years, impedance spectroscopy has emerged as a promising technique in different dental applications, counting the characterization of dental alloys [3], the assessment of the effect of dentine conditioner [4], as well as the discrimination between filling materials and teeth [5], [6].

As far as concerning carious lesion detection, impedance spectroscopy exploits the electrical properties of enamel to reveal structural and compositional changes indicative of early-stage caries. This technique relies on the distinctive demineralization process inherent in caries, which increases the porosity of the tooth structure. The increased porosity allows for conductive fluid infiltration from the oral environment. Through electrical measurements, these alterations can be assessed by identifying the resulting decrease in impedance [7], [8]. Moreover, impedance spectroscopy demonstrates versatility in detecting carious lesions across different tooth surfaces, making it a valuable tool in dental diagnostics [9]. Nevertheless, a comprehensive review [10] reveals that the diagnostic accuracy of select electrical conductance devices, when compared to standard detection methods, lacks robust evidence, with only a limited number of studies specifically addressing dental surfaces and presenting inconsistent results with high-performance variability. Among the few commer-

cially available devices designed for this purpose, CarieScan Pro™ stands out for its popularity. Despite its demonstrated promise, the CarieScan Pro™ device exhibits a classification accuracy that fluctuates significantly according to the different cutoffs, with reported ranges between 52 % and 70 % [11].

Dental caries, also known as tooth decay, is primarily caused by the demineralization of tooth structures due to the removal of mineral ions from hydroxyapatite (HA crystals, $Ca_{10}(PO_4)_6(OH)_2$) in hard tissues like enamel [12]. Untreated demineralization can lead to the irreversible breakdown of tooth structure and the formation of cavities. It is important to note that throughout the day, demineralization and remineralization occur continuously in the oral cavity [13]. Remineralization plays a crucial role in combating dental demineralization and caries progression. It involves the restoration of lost minerals to the tooth structure, helping to repair early-stage carious lesions and prevent further decay [14]. The application on the enamel surface of remineralizing solutions or toothpaste shows a considerable increase in minerals which can aid in reversing the demineralization process and strengthening tooth enamel. Therefore, innovative remineralization agents, such as fluoride, and casein phosphopeptide–amorphous calcium phosphate, are used to restore carious lesions in conservative dentistry as novel non-invasive treatments [15].

Since the chemical and structural composition of enamel changes due to demineralization, it can be detected by Raman spectroscopy. Raman spectroscopy provides quantitative and qualitative chemical information about dental tissue, by providing insights into enamel and dentin composition, enabling early detection of dental caries and variations in tooth structure [16]. The technique's ability to quantify structural information at a nanometer scale and its correlation with other techniques make it a valuable tool for assessing dental demineralization both in-vitro and potentially in-vivo [17]. This technique can be correlated with electrical impedance spectroscopy and with further integration of machine learning, enhances the interpretability of data, paving the way for more accurate categorization and diagnosis.

Despite the limited literature on dental caries detection using artificial intelligence (AI), it demonstrates the significant impact of AI in revolutionizing dental diagnostics. AI, particularly machine learning and deep learning algorithms, has shown promising results in detecting and diagnosing dental caries with enhanced accuracy and efficiency [18]. Most of the studies exploit dental images such as radiographs, photographs, and three-dimensional scans, showing promising results in identifying cavities, especially with bite-wing radiography, that can reach an accuracy of 86.7 % [19]. Additional research explores alternative techniques like Near-Infrared Light Transillumination (NILT) and Optical Coherence Tomography (OCT), applying Convolutional Neural Networks (CNNs) for lesion classification. Results show encouraging accuracy, with CNNs achieving 69 % accuracy in NILT images [20] and up to 89 % in periapical radiographs for detecting caries in premolars and molars [21]. This work improves a novel approach, already presented in [22], that combines impedance spectroscopy with a Single-Perceptron classification system to address the limitations of existing diagnostic tools. The tooth state was confirmed by Raman spectroscopy and Scanning Electron Microscopy (SEM). Focusing on controlled in-vitro demineralization and remineralization processes, we explore the application of innovative nanoparticles to enhance remineralization efficacy. This approach aims to provide a non-invasive, rapid, and reliable method of diagnosing dental caries at early stages, while also monitoring the effectiveness of remineralization using cutting-edge nanoparticles.

II. Sample Preparation and Characterization

To test and validate the proposed approaches experimentally, a comprehensive set of electrical impedance spectra from sound, demineralized, and remineralized human teeth was acquired. The teeth were also characterized by Raman spectroscopy and SEM, providing a comprehensive structural, chemical, and morphological dental state.

A. In-vitro Demineralization and Remineralization Procedure

To minimize the impact of environmental factors on enamel demineralization, this study exclusively utilized frontal incisors extracted within a year. Undamaged incisors were collected with informed consent by expert dentists at the Department of Cariology and Operative Dentistry at the University of Turin in Italy (protocol DS 00071 2018), ensuring they were free from defects, dental caries, or other abnormalities. Post-extraction, teeth were cleaned, stored in a sodium hypochlorite solution 0.5 % w/v (NaClO) to avoid dehydration, and sectioned into comparable sizes. To maintain repeatability in impedance and Raman spectra acquisition, a coating was applied to isolate a $3\ \mathrm{mm} \times 3\ \mathrm{mm}$ window on each tooth's enamel surface. The rest of the tooth surface was covered with a protective coating. Coating-free areas were selected on the coronal vestibular face, ensuring a flat and homogenous surface. A full characterization of the selected spots in terms of surface morphology, electrical impedance spectroscopy, and Raman spectroscopy was conducted to ensure sound tooth surfaces. The exposed tooth surface was then artificially demineralized using a validated protocol [8] involving an acetate buffer with pH adjustments to emulate cariogenic conditions ($4.5 < \mathrm{pH} < 5.5$). The teeth were immersed in the demineralization solution incubated at 38 °C for 96 h without stirring, and subsequently characterized to assess the demineralization state and acquire new impedance and Raman spectra.

To limit carious lesions' progress and restore dental enamel, various innovative preventive measures, including the use of nanocarriers or "nanobubbles" (NBs), have been explored. These nanometer-sized carriers represent a novel method for delivering bioactive substances directly to the target area, offering a promising approach for safe and targeted therapy. Chitosan, a biopolymer known for its minimal toxicity and excellent biocompatibility, was selected for its potential in drug delivery and enamel remineralization, thanks to its ability to bond with dental tissue and slowly release remineralizing

ions [23]. Despite the promising applications of biopolymers like chitosan in dental treatments, challenges in drug release dynamics pose limitations to their application in clinical practice, and more studies are needed [24]. This study employs chitosan-loaded NBs to assess their efficacy in promoting enamel remineralization for treating artificial carious lesions. Thus, to monitor in-vitro remineralization, fluorescent-labeled NBs loaded with various substances were used. Samples were divided into two groups. Fluorescent chitosan-coated NBs loaded with calcium phosphate were applied on a first group of teeth, namely B1, while the second group A1, used as control group, included blank chitosan-coated NBs containing only water, thus with no remineralization effects. NBs solutions were applied by gently scrubbing for $2\ \mathrm{min}$ on the $3\ \mathrm{mm} \times 3\ \mathrm{mm}$ demineralized area with a micro brush. Then the samples were placed in artificial saliva and incubated at 37 °C for 15 days. Subsequently, a new full characterization of the same areas, whose surface is now covered by NBs, was carried out to assess the remineralization process of teeth and acquire electrical impedance spectra, Raman spectra, and SEM images.

B. Morphological Characterization

Morphological characterization of the teeth surface was performed in the small limited window of $3\ \mathrm{mm} \times 3\ \mathrm{mm}$ by means of Scanning Electron Microscopy, before the demineralization procedure, after demineralization, and after the remineralization treatments to monitor surface morphological changes. SEM images (by Phenom™ XL G2 Desktop SEM) of the enamel surface were collected in low vacuum conditions, with an acceleration voltage of $15\ \mathrm{kV}$, at a working distance of $8.5\ \mathrm{mm}$, without any metallization or dehydration of the sample surface. Healthy enamel displays an organized arrangement of HA crystals densely packed giving it a uniform and organic texture as shown in Fig. 1, on the left. On the contrary, observation of demineralized areas (Fig. 1, in the middle) at high magnification reveals increased porosity in demineralized enamel, irregular prism dissolution, and enlargement of intercrystalline spaces. Fig. 1 (on the right) shows the enamel after the remineralization treatment, which presents a layer of mineral formed on the surface, restoring the defect of the enamel prisms showing a comparatively smooth surface. Nevertheless, it is possible to see how the remineralized surface is characterized by a different morphology in respect to a sound natural tooth.

C. Raman Spectroscopy

Raman spectroscopy allows to analyze the molecular structure, biochemical composition, and structural arrangement of organic and inorganic materials in several fields, making it highly relevant also for evaluating dental tissues [25], [26]. For instance, this technique is particularly useful in dentistry for assessing the demineralization effects of bleaching agents and erosive substances on enamel and dentin, or investigating the polymerization process and degree of conversion of resin-based composites and adhesive materials [27], [28]. This technique also enables the monitoring of HA state, which is one of the main components of tooth tissues, allowing the assessment of tooth demineralization and discriminating between healthy and carious tissues. Indeed, the intensity and width of Raman spectral bands, such as the peak at $960\ \mathrm{cm}^{-1}$ associated with the phosphate group PO_4^{3-}, provide insights into the HA's crystallinity and the progression of demineralization.

Raman measurements were carried out using a portable modular spectrometer by BWTEK, equipped with a monochromatic laser ($\lambda : 1064\ \mathrm{nm}$) and a BTC284N spectrometer (measurement range: $100\ \mathrm{cm}^{-1}$ to $2500\ \mathrm{cm}^{-1}$, resolution: $10.56\ \mathrm{cm}^{-1}$), coupled with a CCD sensor. The instrument was connected to a compact microscope (BAC151) that allowed the investigation of the area of interest and the focus of the laser beam with different lenses. The measurements were performed setting a laser power of $225\ \mathrm{mW}$, an integration time of $40\ \mathrm{s}$, acquiring 12 repetitions for each area, employing an 80× microscopic objective (laser spot diameter of about $20\ \mu\mathrm{m}$). For each sample, 3 measurements on three different points of the selected window on the enamel surface were collected, before and after demineralization, and after remineralization treatment.

Fig. 2 shows representative Raman spectra acquired on the enamel surface, in the range between $400\ \mathrm{cm}^{-1}$ to $1800\ \mathrm{cm}^{-1}$. The processing of the Raman spectra was focused in this spectral range since the peak of interest for the demineralization assessment is found at $\sim 960\ \mathrm{cm}^{-1}$, corresponding to the PO_4^{3-} band. This reflects the mineral content of the HA crystal lattice. The observed decrease of HA peak intensity in Fig. 2 is indicative of demineralization-induced alterations in enamel, (blue lines) compared to the sound enamel (green lines). An increase in the peak intensity is mainly attributed to the remineralization treatment (red lines). It is possible to observe how remineralization treatment increases the peak amplitude with respect to demineralized teeth but with a large variability.

D. Electrical Impedance Spectroscopy

Impedance measurements were carried out on the same spot of the tooth: before the in-vitro demineralization, after the demineralization process, and subsequent to the in-vitro remineralization treatment. The purpose was to evaluate the impact of tooth decay and remineralization on the measured impedance. Impedance spectra were collected using an IVIUM-n-Stat potentiostat with a two-electrode configuration and a $0.9\ \%\ \mathrm{w/v}$ NaCl electrolyte solution. A 3D-printed holder kept the tooth stable during testing while platinum wires ($0.1\ \mathrm{mm}$ diameter) were used as electrodes. In particular, the working electrode was placed in contact with the tooth surface while the counter electrode was immersed in the electrolytic solution. Impedance spectra, gathered with a $10\ \mathrm{mV}$ sinusoidal signal across a wide frequency ranging from 10^{-1} Hz to 10^4 Hz, were repeated thrice for consistency. The data revealed significant impedance changes due to demineralization, as well as due to remineralization. As an example, Bode Diagrams shown in Fig. 3 report three

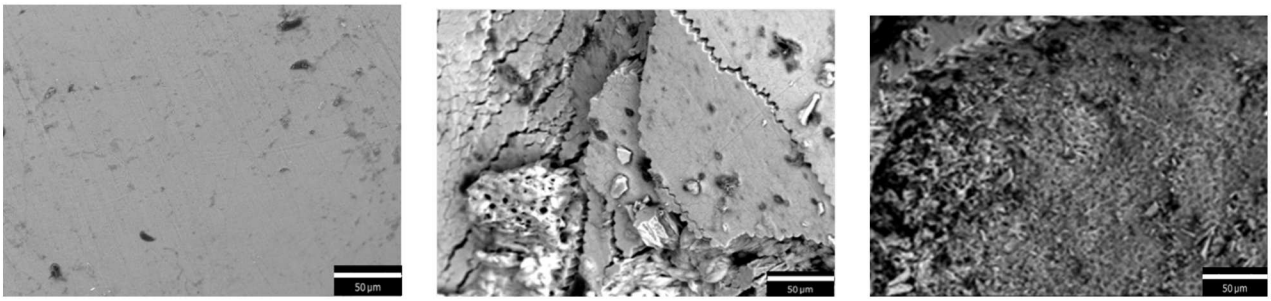

Fig. 1. Scanning electron microscope (SEM) images of sound dental enamel (left), artificially demineralized (center), and remineralized enamel surface (right).

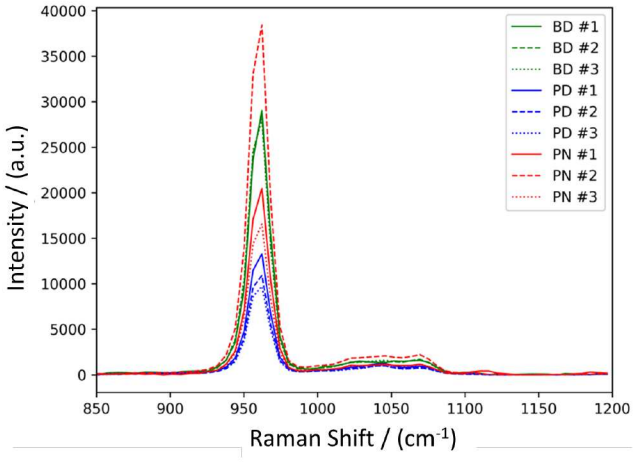

Fig. 2. Raman spectra of enamel, in the range 850 cm^{-1}-1200 cm^{-1} collected on 3 different points of the same tooth before the demineralization (BD, green), after the demineralization (PD, blue), and after the remineralization (PN, red).

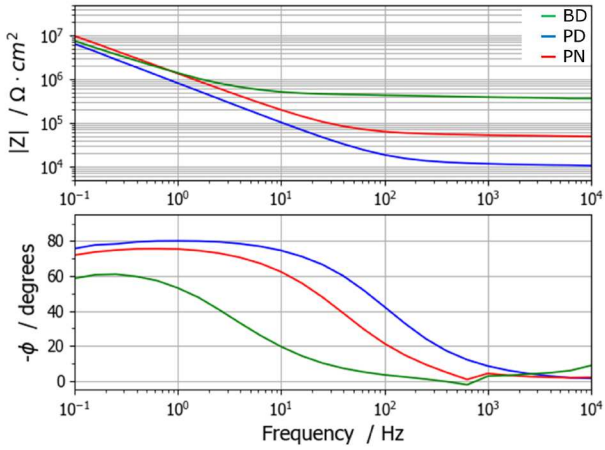

Fig. 3. Impedance spectra collected on a demineralized and subsequently remineralized tooth. Spectra were collected on the same area of tooth surface, before (BD, green), after demineralization (PD, blue), and after the remineralization treatment (PN, red).

measurements on the same sample before demineralization (green line), after demineralization (blue line), and after remineralization (red line). All spectra show a resistive behavior at high frequencies due to the solution resistance and the tooth-solution interface, while low-frequency responses were influenced by the double-layer capacitance at the tooth-probe interface. The demineralization led to a notable decrease in impedance magnitude (indicating increased ion concentration due to heightened surface porosity) and a substantial phase shift. Remarkably, remineralization reversed these changes, moving impedance values toward their original state without, however, totally recovering the values of sound teeth.

III. Classification of Remineralized Teeth

The optimization of these novel remineralization treatments based on NBs is still in progress and, therefore, it is crucial for the researchers to rapidly and non-invasively assess the remineralization treatment effectiveness with a specific measurement device. Moreover, such device can be extremely important in in-vivo experimentation of NBs and real-patient remineralization treatments. Therefore authors, taking advantage of a previously developed classifier for tooth demineralization assessment [22], studied the possibility to automatically assess tooth remineralization state by classifying a single impedance measurement carried out on the treated surface.

A. Single Neuron Classifier

The employed classifier is based on a single-perceptron topology which employs an inverted sigmoid as decision function. The classifier takes as input the impedance phase at a single frequency of 15 Hz and returns the mineralization index going from 0 % for totally demineralized teeth to 100 % for sound teeth. The classifier is configured during training by optimally setting a set of parameters (Input Bias, Weighting Factor, and Decision Function Gain).

B. Classification Performance

The classifier was tested against the dataset collected in the described study which includes about 100 sound and demineralized tooth samples, of which 20 samples were subsequently treated with empty A1 NBs (control group), and other 20 samples were treated with charged B1 NBs. All samples were labelled by experienced operators employing the SEM images and the Raman spectra to confirm the tooth state. A preliminary test for the classification of sound teeth

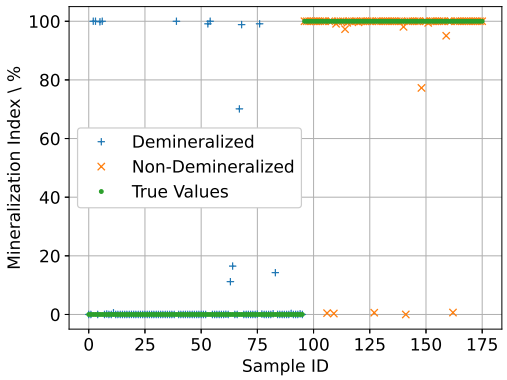

Fig. 4. Results of the preliminary classification test. The graph compares the labelled true values with the classifier predictions both for demineralized and non-demineralized teeth.

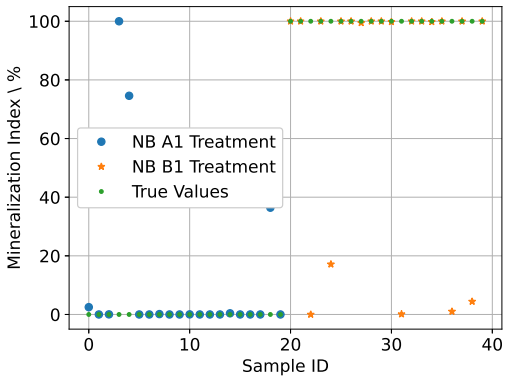

Fig. 6. Results of the NB treatment test. The graph compares the labelled true values with the classifier predictions both for A1 and B1 treatments carried out on demineralized teeth.

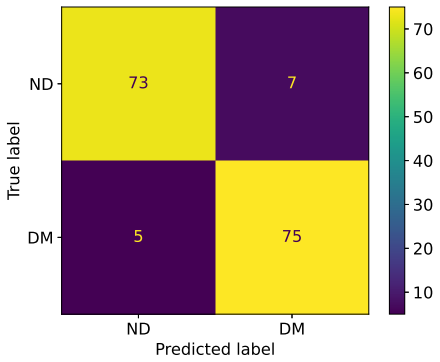

Fig. 5. Results of the preliminary classification test reported as a confusion matrix. Labels ND and DM stay respectively for "Non-Demineralized" and "Demineralized" teeth.

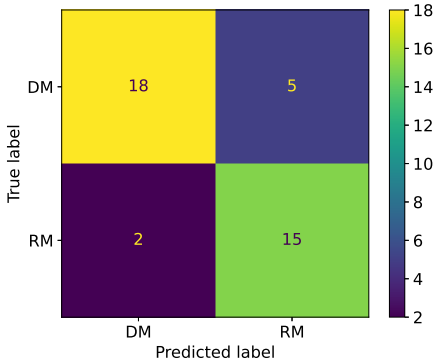

Fig. 7. Results of the NB treatment test reported as a confusion matrix. Labels DM and RM stay respectively for "Demineralized" and "Remineralized" teeth.

(non-demineralized) and demineralized teeth was carried out with the aim of assessing the performance of the classifier. The results are reported in Fig. 4. It is possible to see how most of the samples are properly classified with a total of 15 classification errors over more than 175 samples. Based on these results and choosing a demineralized/non-demineralized threshold of 50 %, classification score indexes are calculated after dataset balancing and reported in the confusion matrix shown in Fig. 5 and in Table I. Classification performances are excellent and well balanced between demineralized and non-demineralized samples, reaching a prediction accuracy of about 93 %.

Subsequently, a classification test was carried out trying to assess the remineralization due to the treatment with NBs. In particular, a dataset composed of 20 impedance spectra collected on samples from group A1 and 20 spectra collected on teeth after the treatment with NBs from group B1 was processed by the same classifier with the aim of assessing if it is possible to discriminate the remineralization state of demineralized teeth from a single impedance phase measurement carried out at a frequency of 15 Hz. All A1 samples remained demineralized after treatment, while the B1 samples properly remineralized. Classification results are shown in Fig. 6, which shows how classification errors for A1 samples are in an amount similar to the preliminary test, while failure rate of the classifier increased on the B1 samples. This is probably due to the fact that remineralized teeth do not completely recover to a sound state, as it was assessed by SEM, Raman spectroscopy, and impedance characterization. Similarly to the preliminary test, classification scores and the confusion matrix have been evaluated and reported respectively in Table I and Fig. 7. Nevertheless, more than acceptable performance is achieved by the classifier with an accuracy of about 83 %.

IV. Conclusion

This study has demonstrated the feasibility of adopting impedance measurements, validated by Raman spectroscopy and SEM analysis, to detect variations in the enamel's structure and composition, indicative of demineralization and remineralization processes. The employed perceptron-based classifier was able to properly differentiate between the various stages

TABLE I
CLASSIFICATION PERFORMANCE OF THE PRELIMINARY TEST (NON-DEMINERALIZED VS. DEMINERALIZED TEETH) AND NB TREATMENT TEST (EMPTY A1 NBS VS CHARGED B1 NBS).

Score	Preliminary Test	NB Treatment Test
Accuracy	0.93	0.83
F1 Score	0.93	0.81
Recall	0.94	0.88
Specificity	0.92	0.78
Precision	0.91	0.75
Negative Predictive Value	0.94	0.90

of enamel integrity, reaching an accuracy of 93 % in recognizing demineralized teeth, and lower accuracy, i.e. 83 %, considering the remineralization treatments. These results not only validate the proposed method as a reliable tool for early detection of dental demineralization but also offer a promising approach for monitoring the effectiveness of remineralization therapies, thereby contributing to preventive dentistry and enhanced oral health care.

REFERENCES

[1] N. Kassebaum, E. Bernabé, M. Dahiya, B. Bhandari, C. Murray, and W. Marcenes, "Global burden of untreated caries: a systematic review and metaregression," *Journal of dental research*, vol. 94, no. 5, pp. 650–658, 2015.

[2] J. D. Bader, D. A. Shugars, G. Rozier, K. N. Lohr, A. J. Bonito, J. P. Nelson, and A. M. Jackman, "Diagnosis and management of dental caries.," *Evidence report/technology assessment (Summary)*, no. 36, pp. 1–4, 2001.

[3] D. Sun, G. S. Frankel, W. A. Brantley, R. H. Heshmati, and W. M. Johnston, "Electrochemical impedance spectroscopy study of corrosion characteristics of palladium–silver dental alloys," *Journal of Biomedical Materials Research Part B: Applied Biomaterials*, vol. 109, no. 11, pp. 1777–1786, 2021.

[4] N. Pradelle-Plasse, F. Wenger, and P. Colon, "Effect of conditioners on dentin permeability using an impedance method," *Journal of dentistry*, vol. 30, no. 5-6, pp. 251–257, 2002.

[5] N. Scotti, A. Comba, M. Cadenaro, L. Fontanive, L. Breschi, C. Monaco, R. Scotti, *et al.*, "Effect of lithium disilicate veneers of different thickness on the degree of conversion and microhardness of a light-curing and a dual-curing cement," *The International journal of prosthodontics*, vol. 29, no. 4, pp. 384–388, 2016.

[6] M. Andrei, C. Pirvu, and I. Demetrescu, "Electrochemical impedance spectroscopy in understanding the influence of ultrasonic dental scaling on the dental structure–dental filling interface," *European journal of oral sciences*, vol. 122, no. 6, pp. 411–416, 2014.

[7] C. Longbottom and M.-C. Huysmans, "Electrical measurements for use in caries clinical trials," *Journal of Dental Research*, vol. 83, no. 1_suppl, pp. 76–79, 2004.

[8] I. Sannino, L. Lombardo, E. Angelini, M. Parvis, P. Arpaia, and S. Grassini, "Preliminary impedance spectroscopy study for carious lesions detection," in *2022 IEEE International Symposium on Medical Measurements and Applications (MeMeA)*, pp. 1–6, IEEE, 2022.

[9] M. Melo, J. L. Sanz, L. Forner, F. J. Rodríguez-Lozano, and J. Guerrero-Gironés, "Current status and trends in research on caries diagnosis: A bibliometric analysis," *International Journal of Environmental Research and Public Health*, vol. 19, no. 9, p. 5011, 2022.

[10] C. O. H. Group, R. Macey, T. Walsh, P. Riley, A.-M. Glenny, H. V. Worthington, J. E. Clarkson, and D. Ricketts, "Electrical conductance for the detection of dental caries," *Cochrane Database of Systematic Reviews*, vol. 2021, no. 12, 1996.

[11] D. Mortensen, I. Hessing-Olsen, K. R. Ekstrand, and S. Twetman, "In-vivo performance of impedance spectroscopy, laser fluorescence, and bitewing radiographs for occlusal caries detection," *Quintessence Int*, vol. 49, no. 4, pp. 293–299, 2018.

[12] E. A. Kidd and O. Fejerskov, *Essentials of dental caries*. Oxford University Press, 2016.

[13] E. A. Abou Neel, A. Aljabo, A. Strange, S. Ibrahim, M. Coathup, A. M. Young, L. Bozec, and V. Mudera, "Demineralization–remineralization dynamics in teeth and bone," *International journal of nanomedicine*, pp. 4743–4763, 2016.

[14] N. B. Pitts, D. T. Zero, P. D. Marsh, K. Ekstrand, J. A. Weintraub, F. Ramos-Gomez, J. Tagami, S. Twetman, G. Tsakos, and A. Ismail, "Dental caries," *Nature reviews Disease primers*, vol. 3, no. 1, pp. 1–16, 2017.

[15] J. Hicks, F. Garcia-Godoy, and C. Flaitz, "Biological factors in dental caries: role of remineralization and fluoride in the dynamic process of demineralization and remineralization (part 3)," *Journal of Clinical Pediatric Dentistry*, vol. 28, no. 3, pp. 203–214, 2004.

[16] J. Silveira, S. Coutinho, D. Marques, J. Castro, A. Mata, M. Carvalho, and S. Pessanha, "Raman spectroscopy analysis of dental enamel treated with whitening product–influence of saliva in the remineralization," *Spectrochimica Acta Part A: Molecular and Biomolecular Spectroscopy*, vol. 198, pp. 145–149, 2018.

[17] I. Otel, "Overall review on recent applications of raman spectroscopy technique in dentistry," *Quantum Beam Science*, vol. 7, no. 1, p. 5, 2023.

[18] S. B. Khanagar, K. Alfouzan, M. Awawdeh, L. Alkadi, F. Albalawi, and A. Alfadley, "Application and performance of artificial intelligence technology in detection, diagnosis and prediction of dental caries (dc)—a systematic review," *Diagnostics*, vol. 12, no. 5, p. 1083, 2022.

[19] L. Megalan Leo and T. Kalpalatha Reddy, "Dental caries classification system using deep learning based convolutional neural network," *Journal of Computational and Theoretical Nanoscience*, vol. 17, no. 9-10, pp. 4660–4665, 2020.

[20] F. Schwendicke, K. Elhennawy, S. Paris, P. Friebertshäuser, and J. Krois, "Deep learning for caries lesion detection in near-infrared light transillumination images: A pilot study," *Journal of dentistry*, vol. 92, p. 103260, 2020.

[21] J.-H. Lee, D.-H. Kim, S.-N. Jeong, and S.-H. Choi, "Detection and diagnosis of dental caries using a deep learning-based convolutional neural network algorithm," *Journal of dentistry*, vol. 77, pp. 106–111, 2018.

[22] I. Sannino, L. Iannucci, L. Lombardo, M. Parvis, A. Comba, P. Arpaia, E. Angelini, and S. Grassini, "Impedance measurements for demineralized tooth lesions assessment," in *2023 IEEE International Symposium on Medical Measurements and Applications (MeMeA)*, pp. 1–6, IEEE, 2023.

[23] M. Kmiec, L. Pighinelli, M. Tedesco, M. Silva, and V. Reis, "Chitosan-properties and applications in dentistry," *Adv Tissue Eng Regen Med Open Access*, vol. 2, no. 4, p. 00035, 2017.

[24] I. S. Bayer, "Controlled drug release from nanoengineered polysaccharides," *Pharmaceutics*, vol. 15, no. 5, p. 1364, 2023.

[25] R. Ramakrishnaiah, G. U. Rehman, S. Basavarajappa, A. A. Al Khuraif, B. Durgesh, A. S. Khan, and I. u. Rehman, "Applications of raman spectroscopy in dentistry: analysis of tooth structure," *Applied Spectroscopy Reviews*, vol. 50, no. 4, pp. 332–350, 2015.

[26] L. Es Sebar, L. Iannucci, Y. Goren, P. Fabian, E. Angelini, and S. Grassini, "Raman investigation of corrosion products on roman copper-based artefacts," *Acta IMEKO*, vol. 10, no. 1, pp. 129–135, 2020.

[27] L. E. Sebar, E. Angelini, A. Baldi, A. Comba, M. Parvis, and S. Grassini, "Nanoindentation and raman spectroscopy measurements on dual-cure luting cement for dental conservative restoration," in *2022 IEEE International Symposium on Medical Measurements and Applications (MeMeA)*, pp. 1–6, IEEE, 2022.

[28] S. Grassini, L. Es Sebar, A. Baldi, A. Comba, E. Angelini, and E. Berutti, "Measurements for restorative dentistry: shrinkage and conversion degree of bulk-fill composites," in *2022 IEEE International Symposium on Medical Measurements and Applications (MeMeA)*, pp. 1–6, 2022.